Climatic Change (2024) 177:123
https://doi.org/10.1007/s10584-024-03773-8

Blue rings in Bristlecone pine as a high resolution indicator of past cooling events

Liliana Siekacz[1] · Charlotte Pearson[2,3,6] · Matthew Salzer[2] · Natalia Soja-Kukieła[4] · Marcin Koprowski[1,5]

Received: 7 December 2023 / Accepted: 19 June 2024 / Published online: 19 July 2024

Abstract

This study develops the use of 'blue rings' (BR), reflecting incomplete cell wall lignification, as a sensitive thermal indicator in bristlecone pine (*Pinus longaeva* D.K. Bailey). Using double-stained anatomical thin-sections, we explore the climatic and topographical constraints governing BR formation by developing a time-series from 83 cores and comparing BR occurrence with the full temporal span of available climatic data (1895–2008 CE). Lignification is temperature-dependent and continues at a cellular level post-radial growth completion. As BRs reflect incomplete lignification, they can serve as a higher resolution and more sensitive proxy for past cooling than previously established tree-growth indicators. Results indicate that blue ring formation is primarily induced by low September temperatures and responds more sensitively to cooling than the well-established frost-ring record. Additionally, the occurrence and intensity of blue rings decreases gradually below the upper tree line. Bristlecone pine BRs are demonstrated to have significant capacity to enhance the reconstruction of past cooling events in North America connected with both localized and hemispheric scale forcing over multi-millennial timescales. Given its unmatched longevity, the species offers an unparalleled potential for Holocene length climate reconstruction. Findings also highlight the potential for blue rings to provide a more nuanced understanding of past temperature fluctuations across multi-millennial timescales.

Keywords Blue rings · Lignification · Dendroclimatology · *Pinus longaeva* · Temperature reconstruction · Wood anatomy

✉ Liliana Siekacz
lilsie@doktorant.umk.pl

[1] Department of Ecology and Biogeography, Nicolaus Copernicus University, Lwowska 1, 87-100, Toruń, Poland

[2] Laboratory of Tree-Ring Research, The University of Arizona, 1215 E. Lowell St, 85721 Tucson, AZ, USA

[3] Geosciences, The University of Arizona, 1040 E. 4Th Street, 85721 Tucson, AZ, USA

[4] Centre for Statistical Analysis, Nicolaus Copernicus University, Chopina 12/18, 87-100, Toruń, Poland

[5] Centre for Climate Change Research, Nicolaus Copernicus University, Lwowska 1, 87-100 Torun, Poland

[6] Anthropology, The University of Arizona, 1009 E. South Campus, 85721 Tucson, AZ, USA

1 Introduction

The environmental constraints of cell wall lignification and the ecological interpretation of varying lignification levels in tree rings require further exploration. A range of early studies using UV microscopic lignin analysis first indicated a connection between the lower lignification of cell walls and lower temperatures (Trendelenburg 1939; Donaldson 1991; Gindl et al. 2000), highlighting the possibility that microscopic study of the lignification process could provide a very real capacity to track seasonal temperature change across a single year's growth. Gindl et al. (2000) went on to demonstrate that lignin concentration in the terminal latewood cells of Norway spruce (*Picea abies* (L.) H. Karst) correlated with autumn (September–October) temperature under alpine growing conditions. Recent advances in wood anatomical thin-section making techniques (Gärtner and Schweingruber 2013) have facilitated the further progress of such studies. In particular, the technique of double staining of transverse micro-sections of tree-ring series with Safranin, which stains red the cell walls which are richer in lignin, and Astrablue, which stains blue the cell walls which are richer in cellulose (coined 'blue rings' by Piermattei et al. 2015), has revealed a faster and more comprehensive way to track the lignification process at a cellular level in long tree ring records (Gerlach 1969; Schweingruber 2007). If lignification is disrupted, the unlignified cells are left behind in the wood structure to create time-series for the development of proxy records. Piermattei et al. (2015) found continuous layers of unlignified axial tracheids both in the earlywood and latewood of Black pine (*Pinus nigra* Arnold) from an advancing tree line in the central Apennines (Italy), and attributed BR occurrence in the last formed latewood cells to a temperature drop at the end of the local growing season (at that growth location, this was the end of October). Crivellaro et al. (2022), in a study covering large latitudinal (40°S and 80°N), and altitudinal (0–6150 m asl) gradients, and analyzing 1770 species of trees, shrubs, and herbaceous plants (with vascular cambium), argues that in the context of global tree line positioning, cell wall lignification is also temperature driven. Montwé et al. (2018) studied BRs and physical damage from frost in lodgepole pine (*Pinus contorta* Dougl. ex. Loud.), revealing that BRs and earlywood frost rings (EWFR) (structural damage characterized by the presence of collapsed/crushed/abnormal tracheids with lateral expansion and displacement of the rays (Glerum and Farrar 1966; Schweingruber 2007), can also be linked to a late initiation of the growing season, an early end of the growing season, and a generally cool growing season. Matisons et al. (2020) analyzed the relationship between BR and minimal summer temperature (July–September) in Scots pine (*Pinus sylvestris* L.) and found it very limited and inconsistent among analyzed trials and provenances. Despite establishing the connection between reduced lignification and temperature, all these studies were limited to relatively short time series and/or low sample depth. Such findings based on short contemporaneous sequences have limited application in a paleoclimatic context. Greater sample depth and longer time-series are required to truly assess the full potential of blue rings as a paleoclimatic proxy.

Upper tree line chronologies from bristlecone pine (*Pinus longaeva* D.K. Bailey) offer potential for constructing far longer than average time-series (Schulman et al. 1955; Schulman 1958) and have well demonstrated potential for multi-millennial reconstructions of temperature, which connect to both regional climate and wider scale volcanic forcing (Salzer and Hughes 2007; Salzer et al. 2014a). In particular, the presence of frost rings in this species has been correlated with the impact of explosive volcanism on climate (LaMarche and Hirschboeck 1984) and has been used to improve chronological

frameworks for the subsequent deposition of volcanic marker horizons in ice core records (Sigl et al. 2015). All of this provides a strong basis to further develop a thermo-lignification record in bristlecone pine, with potential to span much of the Holocene and to expand detailed investigations of volcanic forcing.

Preliminary exploration of BRs in bristlecone pine (Tardif et al. 2020) indicated a likely BR correlation with a late start to the growing season and a cool summer, highlighting the potential for BRs in bristlecone pine to offer a more sensitive proxy for subtle changes in climate due to volcanism and other forcings than the well-established frost-ring record. This study was, however limited by low sample depth and concentrated on only two short, discrete time intervals around 536 and 1965 CE. In order to comprehensively explore the specific climatic parameters, timing, and conditions leading to BR occurrence in bristlecone pine, a comprehensive investigation of BR occurrence across multiple trees and the longest possible time frame for which temperature data are available is required. In this study, BR sequences were created from 83 bristlecone pine cores from the Sheep Mountain/Patriarch Grove area of the Ancient Bristlecone Pine Forest in the White Mountains of California for the period 1895–2014 and 1981–2014, for which respectively monthly and daily climatic data were available. This dataset is the longest and best replicated developed so far with a focus on the investigation of specific climatic conditions leading to BR formation. It also provides the opportunity not only to better evaluate the natural variability of such data, but to present a more comprehensive analysis of the potential for, and limitations of, developing a multi-millennial BR record from bristlecone pine. Additionally, it provides an opportunity to explore the influence of topographic setting in a complex upper tree line ecotone, providing data to better inform future sampling campaigns targeted at producing representative BR chronologies.

The main aims of this study are threefold: (1) to investigate climatic parameters leading to BR formation, (2) to answer if and how elevation and topography modulates the BR record, 3) to evaluate the natural variability of the BR record and assess its paleoclimatic potential and limitations in bristlecone pine.

2 Materials and methods

2.1 Samples and study area

A set of 83 cores were selected from a collection of Great Basin Bristlecone pine (*Pinus longaeva* D. K. Bailey) samples acquired over a series of field campaigns in the Sheep Mountain and Patriarch Grove area of the Ancient Bristlecone Pine Forest in the White Mountains of California (37.5 W, 118.2 N) see Fig. 1.

The trees sampled (Salzer et al. 2014a) spread over an area of roughly 3 km^2 of rugged mountainous terrain consisting of predominantly dolomitic substrate. They cover an elevational transect between 3512 and 3320 m. a. s. l. that is 192 m in vertical distance between the highest and the lowest situated tree. Cores from trees along two distinct transects, (the RW of which have been previously analyzed by (Salzer et al. 2014b) one south facing (SF) and one north facing (NF), were selected to explore the impact of exposure on BR occurrence. Samples from three other bristlecone pine chronologies from the White Mountains: Cottonwood Upper (CWU), Sheep Mountain (SHP) and Patriarch Lower (PAL), were also selected in order to extend the vertical distance covered by the samples to assess any

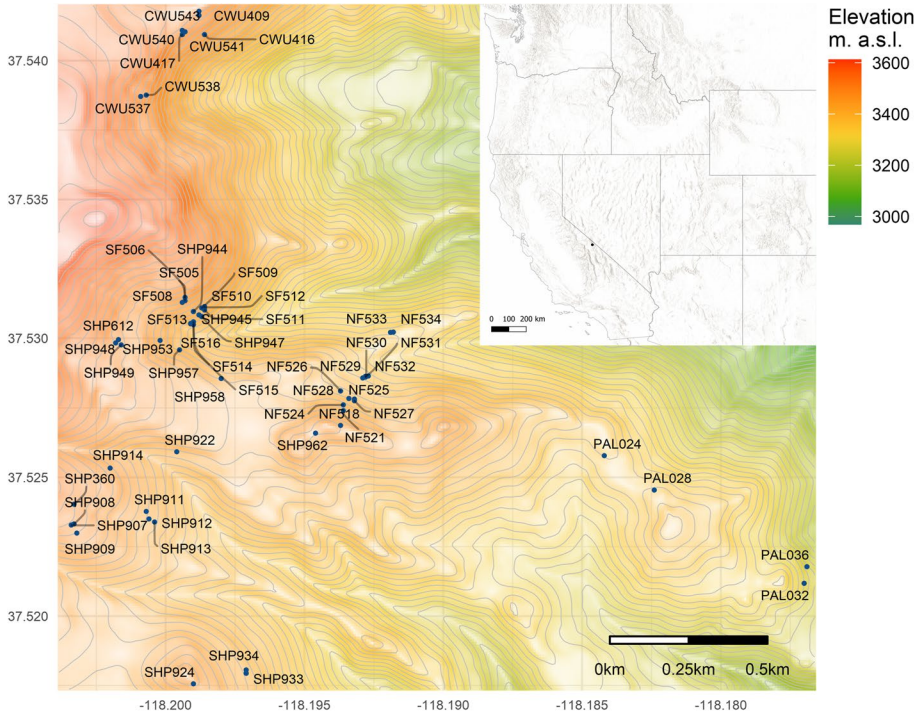

Fig. 1 Locations of sampled trees in the White Mountains of California. Inset map shows the general location of the study area in the western United States. Please note that trees SHP972 and SHP975 are not shown on this map, as these were located circa 3 km to the north from the main group of sampled trees shown

impact of altitude or distance from upper tree line on BR formation. These cores were also assigned as predominantly south or north facing based on the topographic position of the sampled trees.

To explore BR continuity around the stem where possible, we included two cores per tree. The strip-bark nature of bristlecone growth is such that for more mature trees there are often only a few sampling locations on the tree where the cambium is active (Brunstein 2006; Boyce and Lubbers 2011), imposing some limitations on the sampling strategy. Suitability for sectioning also required selection of cores with relatively consistent internal structure to facilitate effective sectioning of the material to avoid any distortion of the tracheid wall dimensions. The final selection of 83 cores suitable for this study includes 44 cores representing double sampled trees and a further 39 representing a single sampling from a tree (Table S1).

2.2 Laboratory preparation

Cores used for this study were previously air dried, glued into wooden core mounts, sanded, and measured following standard dendrochronological procedures (Stokes 1996; Salzer et al. 2014b). For this study, cores were separated from their mounts by soaking in a tray filled with near boiling water until they detached from the core mounts. Subsequently

each core was cut into shorter 4-6 cm long diagonally overlapping segments that could be reassembled with ease to perform accurate cross-dating on the finished sections. The cores were not cut into equal length segments because each core was individually assessed under the microscope to ensure maximum ring overlap on both sides of the split. The order of the sectioned pieces was noted to enable final reassembly of each core when the sectioning process was over. All core elements were next cut into c.10-15 µm thick thin-sections using a GSL1 microtome (Gärtner et al. 2014).

Thin-sectioning was followed by staining in a mixture of Safranine and Astrablue to reveal lignified cell walls in red and emphasize underlignified cell walls in blue. Stains were prepared following the procedure by Gärtner and Schweingruber (2013), where 0.5 g of Astrablue powder is dissolved in 100 ml of distilled water and 2 ml acetic acid, and 0.1 g of Safranin powder is dissolved in 100 ml of distilled water. Finally both stains were mixed in a 1:1 proportion. Each thin-section was placed in the stain bath for 3–4 min, after which it was washed with water and then ethanol at gradually increasing concentrations of 50%, 75%, 99,8% to remove the surplus stain from intercellular spaces and to dehydrate the section. Finally, each section was embedded in Canada Balsam under a cover glass and oven dried for 24 h in 60 °C. Laboratory preparation of 83 cores resulted in 612 permanent thin-sections. These were then digitized to facilitate ring width measurement and cross-dating. Thin-sections were photographed with a digital camera (CANON EOS 700D) coupled to a microscope under 40 times magnification. In total 29,105 high resolution pictures were taken, which were subsequently stitched in PTGui software (http://www.ptgui.com) to create high-resolution images of entire thin-sections. A control photo of an according scale was taken for each microscope magnification to ensure accurate analysis. Care was taken to achieve a representative overlap (20–30%) between single photos to secure reliable stitching results. Finally, ring widths of thin-sections representing every core were measured in ImageJ software (https://imagej.nih.gov/ij/index.html), and ring width sequences visually cross-dated and confirmed using CDendro software (http://www.cybis.se/forfun/dendro/) against the previously dated cores. The cell structure of the sections was surveyed using both the high-resolution digital images and the stained slides at 40×and 100x magnification. Underlignified tracheids (Fig. 2), were noted and assigned calendar dates for each observed BR. Earlywood Frost Rings (EWFR) and Latewood Frost Rings (LWFR) were also observed and assigned calendar dates.

2.3 Climate indices and statistical analysis

To assess the association between temperature and BR occurrence, mean-monthly temperature data were obtained for the grid pertaining to Sheep Mountain (Location: 37.5470 lat, -118.2179 lon, Spatial resolution 4 km, PRISM Climate Group, Oregon State University, http://prism.oregonstate.edu). Mean-monthly temperatures in the PRISM (Parameter-elevation Regressions on Independent Slopes Model) dataset are available for the period starting in January 1895; therefore, our analysis covers years 1895–2014 (2014 being the latest year in which our group of samples were collected). Our complete dataset, unusually large for thin-section analysis, with a sample depth of 83 cores, and temporal coverage of 120 years (for which temperature data was available), allowed us to implement a modeling approach to analyze the association between BRs and temperature. Our dataset consists of a time-series (non-independent setting) representing observations within individual cores that vary in their sensitivity to BR formation. Therefore we decided to fit a generalized linear mixed-effects model (GLMM), to account for these dependencies in the

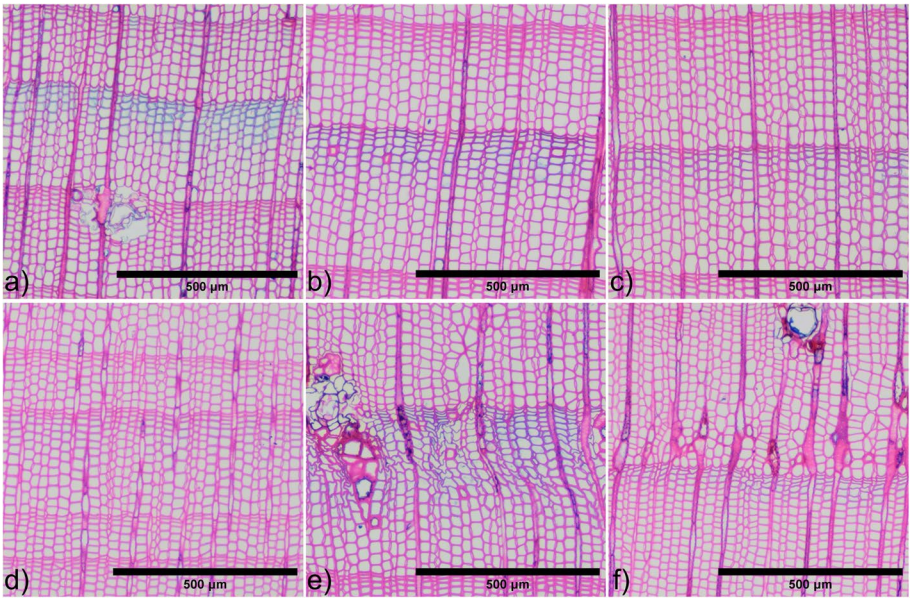

Fig. 2 Observed anatomical abnormalities: **a**) blue ring type 1 (BR-1), **b**) blue ring type 2 (BR-2), **c**) blue ring type 3 (BR-3), **d**) blue ring type 4 (BR-4), **e**) BR-1 along with deformed cells of late-wood frost ring, **f**) BR-3 followed by a lesser early-wood frost ring. Please note the difference between cell distortion in a) which occurred during sectioning due to the reduced strength of the cell walls due to lower lignin content, and the frost deformation of cells during life of the tree in e) and f). It is possible to clearly distinguish between the two effects through microscopic examination of the uncut sample, and the fact that procedural deformation produces a more uniform effect at a cellular level

data. We treat each core as a random effect, allowing the intercept of the model to vary among cores. The response variable is binary, representing the absence (0) or presence (1) of BR in a particular year, in a particular sample. The independent variables are mean-monthly temperatures of respective years, and the vertical distance from the upper tree line in meters (hereafter referred to as DTL). Samples analyzed are from trees growing on predominantly southerly or northerly exposed slopes of the temperature determined upper tree line (Bruening et al. 2017). Upper tree line elevation differs on both these slopes, so the distance from the respective upper tree line elevation of 3511 m on the southern slope, and 3475 m on the northern slope (Salzer et al. 2014b) was calculated for each core analyzed. To account for the independence of observations in our model we included only one sample per tree, resulting in a sample depth reduction to 61 individual cores. In order to fit the model, we used a manual step-wise, step-down, backward elimination procedure. We initially constructed the model with all available explanatory variables (mean temperature for every month and DTL); subsequently, we built a model retaining only variables significant at $p < 0.01$ from the first model. The final model included 7 significant explanatory variables: mean monthly temperatures of February, April, June, August, September, October, and DTL. Data analysis was conducted in R, v. 4.1.3 (R Core Team, 2024), using the package "lme4" for mixed modeling (Bates et al. 2015). The model specification was as follows: BR_event ~ feb_tmean + apr_tmean + jun_tmean + aug_tmean + sep_tmean + oct_tmean + DTL + (1|core) and the model was estimated using ML and BOBYQA optimizer.

Mean-daily temperature data were obtained for the grid pertaining to Sheep Mountain (Location: 37.5470 lat, -118.2179 lon, Spatial resolution 4 km, PRISM Climate Group, Oregon State University, http://prism.oregonstate.edu) for the full period available, that is 1981–2014, to explore the association between BRs and daily temperatures.

2.4 Topographic indices and statistical analysis

In order to further assess the association between BR occurrence and topographic variables, DTL and exposure, we calculated BR frequency per tree for the period 1793–1998, the longest period continuously covered by the highest number of samples (61 in total). We then applied simple linear regression between BR frequency and DTL, and used the non-parametric Mann–Whitney U test to compare cores from southerly- and northerly-exposed trees. BR frequency was calculated per tree, not per core in this case, because two cores coming from the same tree are influenced by the same DTL and slope exposure.

In order to assess if trees growing in cooler topographic locations might be more susceptible to record BRs driven by colder temperatures (as suggested by Bunn et al. 2011; Bruening 2016; Bruening et al. 2018) as compared to trees in surrounding areas, topoclimate variables—mean-monthly temperatures derived by Bruening et al. (2017, 2018) for each tree location were used. We again used the non-parametric Mann–Whitney U test to check for significant differences in topoclimate variables between BR-recording and non-recording trees in years of BR formation.

3 Results

3.1 Blue ring typology

Careful examination allowed us to develop a classification of blue ring intensity (Table 1) for use in this study, based on observations of the full range of variability, such as: numbers of rows of under lignified tracheids; the degree of lignification of the tracheid walls; the thickness of the latewood cell walls compared to the latewood of surrounding rings: and the overall intensity of the blue color ensuing from the proportion of underlignified cell walls.

The BRs that we observed in this study appear exclusively in the latewood, predominantly in its outermost part consisting of the 2–5 outermost cells of a radial file. A few of the most intensive examples included blue in up to 50% of ring width, and these were usually coupled with LWFRs (Fig. 2e).

In cases of particularly strong BRs (BR-1, BR-2) tracheid shapes can be distorted during thin-section preparation because of lowered lignin content (which provides rigidity and mechanical strength). In such cases, careful microscopic examination can distinguish strong BRs from frost rings, because in BRs only the tracheid and ray shapes are distorted during microtome preparation, whereas FRs are also characterized by lateral expansion and displacement of rays (Fig. 2).

In total (1895–2014, 9357 rings), we identified only 203 BRs (0.022) of which BR-1: 0 (0.0), BR-2: 18 (0.002), BR-3: 67 (0.007), BR-4: 118 (0.013). BR-1 type are extremely rare and in fact present only in very strong BR years in the earlier part of the dataset, for which temperature data were not available for comparison. In this dataset, frost rings occur

Table 1 BR intensity classification

Blue Ring Type	Characterization	Example shown
BR-1	Strongly blue in section, multiple rows of underlignified tracheids, complete sections of tracheid walls are underlignified, underlignified latewood cell walls are visibly thinner compared to the latewood of the surrounding rings, and in some cases the initiation of cell wall lignification can be observed in cell wall corners (pink). In some instances they appear coupled with LWFRs	Figure 2a,e, Fig. S1a
BR-2	Less blue in section compared to type 1, the lignification process progressed further from cell corners with only the inner portion of the tracheid walls appearing blue	Figure 2b, Fig.S1b
BR-3	Less blue in section compared to type 2, with only the very thin innermost cell wall part appearing blue	Figure 2c,f, Fig.S1c
BR-4	Slight bluish tint in section visible in the latewood cells, present in the same year in at least 2 samples*	Figure 2d, Fig.S1d

*A similar effect could also potentially be produced by insufficiently washed-out stain from intercellular spaces. This type was only assigned where the effect was present in the same year in at least two samples, as it is unlikely for two separate samples to independently show this stain-washing effect in the same year

even more rarely, only a single LWFR was observed in the period of analysis (0.0001), and EWFR in 19 rings (0.002).

Our data indicate that BR and EWFR in bristlecone pine are independent markers, with only 2 EWFRs out of 19 following BRs. Blue rings in bristlecone pine at our growth locations form in years with lower-than-normal temperatures during the late part of the growing season, while EWFRs probably mark early cambial reactivation and cold snaps at the beginning of the growth season. A Mann–Whitney U Test was performed on mean monthly temperatures for the period 1895–2014 and confirmed that mean May temperatures were significantly higher ($p = 0.002$) (Table S2, Fig. S2) in years with EWFRs. Such early-season warmth possibly induces an earlier-than-normal onset of cambial activity and resultant frost damage from subsequent spring cold snaps. Analysis of daily temperatures for the period 1981–2014 confirms that in EWFR years (1984, 1992, 2007) minimal daily temperatures rose above 0°C already in May and were later followed by period of below-zero temperatures likely leading to the observed frost damage (Fig. S3).

3.2 Temperature constraints of blue ring formation

Model input for the period 1895–2014 includes 61 samples from independent trees, in total 6848 observations. The model's total explanatory power is substantial, with a conditional $R2 = 0.796$, and the part related to the fixed effects (marginal R2) is 0.558. The model fit parameters indicate an optimal fit. Both the C-value (0.9681743) and Somers' D_{xy} (0.9363487) show a good fit between predicted and observed occurrences of BRs. If the C-value is 0.5, the predictions are random, while the predictions are perfect if the C-value is 1. C-values above 0.8 indicate real predictive capacity (Baayen 2008). Somers' D_{xy} is a value that represents a rank correlation between predicted probabilities and observed responses. Somers' D_{xy} values range between 0, which indicates complete randomness, and 1, which indicates perfect prediction (Baayen 2008).

The model indicates that mean-monthly temperatures in February, April, June, August, September, and October significantly influence BR formation, along with distance from upper tree line (DTL) (Table 2).

The higher the average monthly temperature in February, the higher the odds of a BR forming later in the year (Table 2, Fig. 3a). Whereas, lower temperatures in April raise the probability of lignification being disrupted later in the growing season, leaving behind an underlignified band of cells in the latewood of that particular year (Table 2, Fig. 3b).

We observe a negative relationship between June mean temperature and BR formation (Table 2, Fig. 3c); the cooler June is, the higher the odds of BR formation. It is possible that June, as the month when cambial activity starts, might also be partly defining how long cambial activity can be sustained, that is, the length of the growing season. A cool June may lead to the latest formed tracheids being challenged to fully lignify when cold snaps in September and/or October arrive. This interplay is clear when we look at the predicted likelihood of BR formation in September and October under different temperature scenarios for June (Fig. S5). Lower temperatures in June delay the onset of xylogenesis. Thus, the lignification of latewood tracheids could still be ongoing in September/October when colder temperatures arrive, disrupting the lignification completely and leading to the formation of a BR.

We do not observe any significant relationship between mean July temperature and BR occurrence. We suggest that, however much cooler, temperatures in July across our period of

Table 2 Parameters of generalized linear mixed-effects model (GLMM)

Predictors	BR event			
	Log-Odds	*CI*	*Statistic*	*p*
(Intercept)	8.36 ***	6.42 – 10.31	8.44	3.266e-17
February mean temp	0.26 ***	0.14 – 0.37	4.29	1.817e-05
April mean temp	-0.33 ***	-0.45 – (-0.21)	-5.26	1.406e-07
June mean temp	-0.82 ***	-0.97 – (-0.67)	-10.57	3.976e-26
August mean temp	-0.39 ***	-0.55 – (-0.23)	-4.83	1.396e-06
September mean temp	-1.12 ***	-1.32 – (-0.93)	-11.29	1.514e-29
October mean temp	0.15 ***	0.07 – 0.24	3.44	5.799e-04
DTL	-0.03 **	-0.04 – (-0.01)	-3.04	2.361e-03
Random Effects				
σ^2	3.29			
$\tau_{00\ symbol}$	3.82			
ICC	0.54			
$N_{\ symbol}$	61			
Observations	6848			
Marginal R^2 / Conditional R^2	0.558 / 0.796			
AIC	856.487			

* $p < 0.05$ ** $p < 0.01$ *** $p < 0.001$

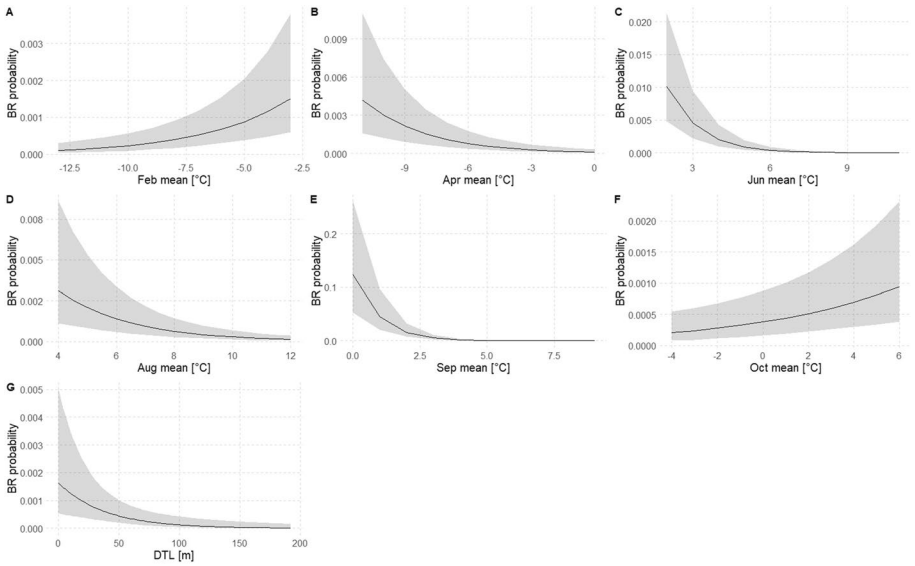

Fig. 3 Generalized linear mixed-effects model (GLMM) results presented as predicted probabilities of BR formation for each predictor significant in the model, plotted along observed ranges of predictors. BR probability is shown according to: **a**) February mean temperatures, **b**) April mean temperatures, **c**) June mean temperatures, **d**) August mean temperatures, **e**) September mean temperatures, **f**) October mean temperatures, **g**) DTL. Please note the highest effect of September mean monthly temperature on the probability of BR formation. Note the different y-axis in each subplot

study (1895–2014) never dropped to the level where they might disrupt the lignification process of newly forming early-wood tracheids. This is further supported by the observation that we also do not see BRs in earlywood across our period of study, just in the last tracheids of the latewood towards the very end of the growth season.

The effect of the mean temperature in August is negative (Table 2, Fig. 3d), cooler temperatures increase the likelihood of BR occurrence.

Model results indicate that the strongest relationship exists between September temperatures and the occurrence of BRs (Table 2, Fig. 3e). On average, cambial activity in bristlecone pine ceases when mean daily temperatures drop below 6 °C (Ziaco et al. 2016). This threshold is normally reached at our site by approximately the 17th of September (Fig. S6). While this date will vary somewhat, we can extrapolate that the production of new tracheids stops and lignification of the lastly formed cells occurs around mid-September.

Mean October temperatures appear to have a positive effect on the likelihood of BR occurrence (Table 2, Fig. 3f). A 1 °C increase in mean October temperature increases the odds of BR formation by 16%. In some years, favorable conditions for cambial activity, with average daily temperatures above 6 °C, can still occur for some part of October (Fig. S6), effectively extending the time window when lignification can occur into periods where sudden temperature drops are likely, if not inevitable. In this scenario, late cambial activity leads to a late start to the lignification process and a subsequent thermally induced lignification disruption and the formation of a BR. Such situations are not very frequent and therefore the effect of October temperatures in our model is relatively low. We suggest that the influence of June and October mean temperatures impacts BR formation by effectively either delaying or extending the time window of favorable conditions for xylogenesis.

There are cases when BR formation is most probably induced by short temperature decreases at scale of a couple of days as observed by Piermattei et al. (2015). This kind of short-term temperature variation is not well captured by average monthly temperatures. Daily temperature records for the study area are only available from 1981 onwards (PRISM), and for this most recent period in our dataset, we observed only two BR events, one in 1982 (17 out of 82 samples) and one in 1998 (4 of 82 samples). We compared the relationship of BR occurrence with mean daily temperatures during these two event years (Fig. S7). The result for the 1982 growth season indicates that BR formation was mainly influenced by temperature in June and September. A short growth season characterized 1982, with < 6 °C mean daily temperatures occurring until 11th of July and cold snaps with below-zero mean daily temperatures still occurring up to the 1st of July. The growth season ended with temperatures dropping below 6 °C on the 11th of September. In contrast, the beginning of the growth season in 1998 was not characterized by such harsh conditions, as indicated by the weaker BR signal present in only 4 out of 82 upper tree line (DTL-14 ± 15 m) samples. Cambial activity likely started around the 19th of June; however, temperature dropped below 6 °C for a couple of days beginning on the 10th of September, which might have induced a lignification shutdown and the limited BR formation seen in the dataset.

Modeled temperature results also revealed a weak but significant negative effect in relation to distance from the upper tree line (Table 2, Fig. 3g), with a one meter increase in DTL decreasing the odds of BR formation by 3%. This potential topographic influence was further explored using different techniques.

3.3 Topographic influence on BR occurrence

We observe a significant ($p=0.01$) negative relationship between BR frequency and DTL (Fig. S4). Although the observed relation explains only 9% in the variance of the dataset, DTL constitutes the strongest common topographic constraint of BR occurrence. A non-parametric Mann–Whitney U test between BR frequency on southerly and northerly exposed slopes shows that there is no significant ($W=435$, $p=0.83$) difference between the distribution of BR frequencies on both exposures (Fig. S4). We therefore found no evidence for exposure influencing the trees' susceptibility to BR formation.

Results across 79 cores (1793–1998), arranged in an ascending order of DTL show that the further below the tree line the tree is located, the less severe the temperature impact of a given event (Fig. 4). We observe a buffering effect with distance below the upper tree line, which is balanced against the severity of the cold snap. More extreme low-temperature departures result in stronger and more BRs in the higher portion of the elevational transect, with weaker and fewer BRs present in trees further down from the upper tree line.

Examining the pairs of cores from the same tree (Fig. S8), we can observe that BRs are often not continuous around the stem. Usually, one of the pair of cores records more BRs and of higher class than the other. This may be due to stem exposure, where the side of the trunk that is not exposed to direct solar radiation remains slightly cooler than the sun-exposed side, and thus the non-exposed side is prone to record more and stronger BRs.

We performed non-parametric Mann–Whitney U test between BR-recording and non-recording trees in every BR year for DTL and mean monthly temperatures (topoclimate

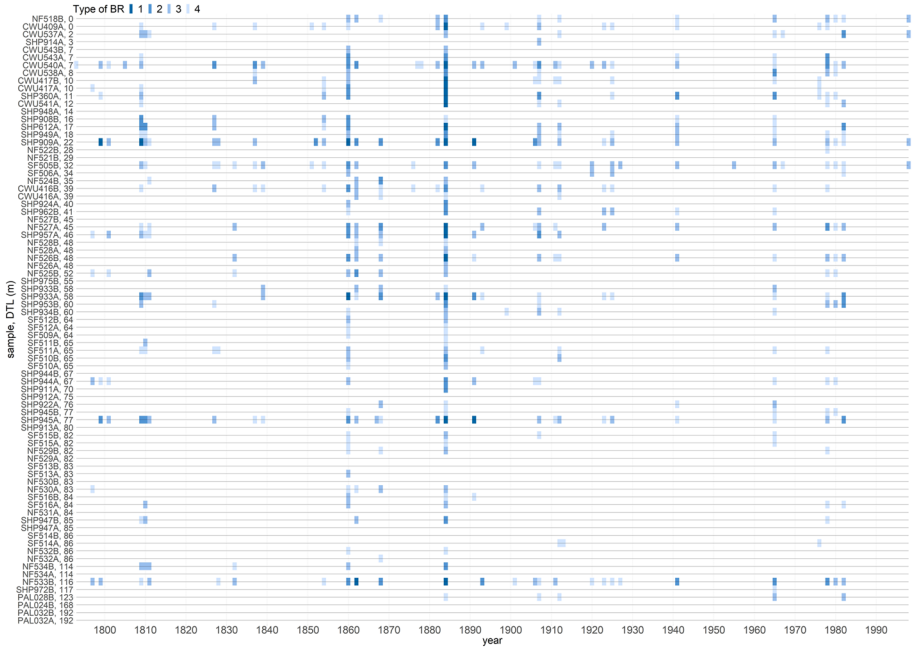

Fig. 4 BR chronology of 79 cores continuously covering the period 1793–1998, arranged in an ascending order of DTL. Please note that the further below the upper tree line the tree is located the fewer BRs it forms and that the BRs formed in a particular year become less intense with increasing DTL

variables derived by Bruening et al. (2017)) of each month for the period 1793–1998 continuously covered by 61 trees (Table 3). We identified 47 BR event years (1793, 1797, 1799, 1801, 1805, 1809, 1810, 1811, 1818, 1827, 1828, 1832, 1837, 1839, 1851, 1852, 1854, 1860, 1862, 1868, 1876, 1877, 1878, 1882, 1884, 1891, 1893, 1899, 1901, 1906, 1907, 1911, 1912, 1913, 1920, 1923, 1925, 1927, 1941, 1955, 1965, 1967, 1976, 1978, 1980, 1982, 1998). We observed significant ($p <= 0.01$) differences only for June in 1907, July 1907 and November 1868 and for DTL in 1907, 1941, 1809, 1837. This shows that the BR sensitivity of particular trees cannot be sufficiently explained by obtained topoclimate variables.

Table 3 Results of the Mann–Whitney test (two-sided) of differences in DTL and topoclimatic variables calculated for each tree location between BR-recording and non-recording trees for 47 BR event years between 1793–1998. The median and interquartile range (IQR) are indicated. Note that the number of observations per group varies for each year analyzed. Only results significant at least at the level of $p \leq 0.05$ are listed, results significant at $p \leq 0.01$ are bolded

Variable	Year	n BR	n non-RB	Median (IQR) BR	Median (IQR) non-BR	*p* value
DTL	1907	26	34	35.5 (11–60) m	67.5 (37–84) m	**0.002**
	1941	16	44	20 (7–45) m	64 (37–83) m	**0.005**
	1809	22	36	27 (11–60) m	66 (40–83) m	**0.007**
	1837	8	51	16 (7–32) m	60 (34–83) m	**0.008**
	1998	4	55	12 (0–22) m	58 (29–82) m	0.014
	1854	9	50	17 (11–32) m	62 (35–83) m	0.016
	1925	13	47	32 (11–41) m	64 (35–83) m	0.023
	1884	44	14	48 (16–70)m	81.5 (34–117)m	0.033
	1882	7	52	22 (0–58)m	60 (29–83) m	0.034
	1827	10	49	27 (16–60) m	60 (34–83) m	0.045
January temperature	1868	16	43	-6.7 (-6.9-(-6.1)) °C	-5.8 (-6.5-(-5.5)) °C	0.013
	1862	16	43	-6.7 (-6.9-(-5.9)) °C	-5.8 (-6.7-(-5.5)) °C	0.047
	1811	10	48	-6.8 (-6.9-(-5.8)) °C	-6.1 (-6.7-(-5.5)) °C	0.048
April temperature	1907	26	34	-2.3 (-2.5-(-1.9)) °C	-2.0 (-2.3-(-1.8)) °C	0.033
May temperature	1907	26	34	1.7 (1.5–2.0) °C	1.9 (1.7–2.1) °C	0.019
	1809	22	36	1.7 (1.5–1.9) °C	1.9 (1.7–2.1)°C	0.028
June temperature	1907	26	34	7.0 (6.8–7.2) °C	7.2 (7.1–7.5) °C	**0.007**
	1809	22	36	7.0 (6.8–7.2) °C	7.2 (7.0–7.5) °C	0.026
July temperature	1907	26	34	10.8 (10.6–10.9) °C	11.0 (10.8–11.2) °C	**0.005**
	1809	22	36	10.8 (10.6–10.9) °C	11.0 (10.7–11.2) °C	0.012
August temperature	1907	26	34	10.7 (10.4–10.8) °C	10.9 (10.7–11.0)°C	0.010
	1809	22	36	10.7 (10.4–10.8) °C	10.9 (10.7–11.0) °C	0.016
September temperature	1907	26	34	7.1 (6.9–7.4) °C	7.4 (7.1–7.6) °C	0.024
November temperature	1868	16	43	-1.7 (-2.1-(-1.2)) °C	-1.0 ± (-1.7-(-0.7)) °C	**0.006**
	1862	16	43	-1.7 (-2.1-(-1.1)) °C	-1.0 (-1.7-(-0.7)) °C	0.025
	1811	10	48	-1.8 (-2.1-(-1.1)) °C	-1.2 (-1.7-(0.8)) °C	0.046

4 Discussion

4.1 Blue ring typology

At a cellular level, our observations of the lignification process were compatible with previous studies (Saleh et al. 1967), which observed that cell corners in the primary wall lignify first and subsequently lignification continues in the middle lamella of the radial and then tangential walls. Results in this study demonstrate that in varying stages of incomplete lignification, radial walls are visibly more strongly lignified than tangential walls (Fig. S1).

BR were present only in the latewood portion of the ring for our time-series (1793–2014) as observed by Montwé et al. (2018) and Matisons et al. (2020), but not by Piermattei et al. (2015) who reported BR in both the terminal portion of the ring and within the earlywood portion.

The fact that in our dataset, LWFR occur less frequently than EWFR, is in contrast to earlier studies, which report EWFR to occur less frequently than LWFR in bristlecone (LaMarche 1979; LaMarche and Hirschboeck 1984; Brunstein 1995). However, this difference may originate from differing sample preparation in earlier studies, where frost rings were noted on polished core surface, and less obvious EWFRs might have gone unrecognized. Detailed microscopic analysis based on thin-sections allows us to recognize even the slightest abnormalities in wood structure.

Our analysis shows that BR and EWFR are independent markers of two separate events. This is contrary to indications by Montwé et al. (2018), on a far more limited dataset, that BRs capture a cold event at the end of the growing season which leads to cambial damage and irregular growth upon re-activation in the following spring. In bristlecone pine at our growth locations, BRs form in years with lower-than-normal, but not below freezing temperatures during the late part of the growing season that are sufficient to cease lignification without damaging the cambium. In contrast EWFRs probably mark early cambial reactivation and cold snaps at the beginning of the growth season.

Studies of lodgepole pine (*Pinus contorta* Dougl. ex. Loud.) (Montwé et al. 2018) and Scots pine (*Pinus sylvestris* L) (Matisons et al. 2020) have reported higher proportions of BRs and FRs than this study. While this could be a species specific difference, the trees used in these earlier studies were not growing in their natural proveniences and so may have been over sensitized. However, Greaves et al. (2022) also reported higher BR proportion for Scots pine (*Pinus sylvestris* L) growing within its seed source location and far from the thermal limits of Scots pine growth. As bristlecone pine is highly adapted for survival in its marginal habitat, we conclude that BRs are formed very rarely, only during highly extreme conditions, and the bristlecone BR record therefore constitutes a more reliable record of years with adverse climatic conditions. Both earlier studies (Montwé et al. 2018; Matisons et al. 2020) also reported higher proportions of BRs compared to frost rings, which is in agreement with our results. This implies that BRs represent a more sensitive reaction of tree growth to adverse thermal conditions than FR, which require below freezing temperatures to form. This is particularly important in the context of bristlecone pine given the previously described and longstanding association of FRs with explosive volcanism (LaMarche and Hirschboeck 1984; Brunstein 1996; Salzer and Hughes 2007). Blue ring records might allow early or late growth season distinction for specific eruptive events (LaMarche and Hirschboeck 1984; Gurskaya 2014; Barbosa et al. 2019). A long BR record could augment FR records of past

eruptions (Piermattei et al. 2020; Büntgen et al. 2022) and could considerably enhance paleoclimatic and cultural histories related to eruptive events as well as their influence upon regional circulation patterns.

We did not observe any relationship between juvenility and an increased probability of BR formation, as noted by Matisons et al. (2020) and Montwé et al. (2018), related to weaker insulation of the cambium (Payette et al. 2010; Montwé et al. 2018), the lower height, and weaker heat absorption of smaller trees (Kidd et al. 2014) because all cores used in this study came from mature trees.

4.2 Temperature constraints of blue ring formation

Connections between mean-monthly June, August, September, and October temperatures and BR occurrence confirm preliminary observations (Montwé et al. 2018; Matisons et al. 2020; Tardif et al. 2020) that BRs form due to late initiation of the growing season, an early end of the growing season, and a generally cool growing season. Although limited by the lack of longer sequences of daily temperature data, we were also able to support the suggestion made by Piermattei et al. (2015), that there is a connection between short-term temperature decreases (at the scale of several days) at the end of the growing season and the occurrence of BRs, based on our observations of the 1982 BR event. Further analysis of the relationship between short-term temperature decreases and BR formation is necessary to fully confirm this association in settings where daily temperature records are available.

We were also able to develop a deeper understanding of the previously hypothesized temperature response, revealing some additional subtleties to be expanded on in future studies. The observed connection between February and April mean temperatures and BR occurrence seems initially surprising, as the cambial activity of bristlecone pine in other growth locations has been observed to start when mean daily temperatures reach around 6 °C (Ziaco et al. 2016), which, at our sampling site occurs on average around 13th of June (Fig. S6). Therefore, the lignification process, the last phase of xylogenesis, should not be directly affected by temperatures occurring before the onset of the cambial activity itself. However, ecophysiological models of the onset of cambial activity can potentially explain this connection. Delpierre et al. (2019) compared various models, including temperature threshold, temperature and photoperiod thresholds, heat-sum, chilling influenced heat-sum, and regression line models, and found that a chilling influenced heat-sum model provides the highest accuracy predictions of the onset of cambial activity. This was based on a large observational dataset spreading through a broad altitudinal, and latitudinal gradient of four different coniferous species. The model considers the complex interplay of chilling and forcing temperatures in interaction with the photoperiod and attempts to address the influence of ecodormancy and endodormancy phenological phases on the resumption of cambial activity. During the endodormancy phase, cambial activity is prevented by the tree's internal physiology, even if favorable external conditions arise the tree does not respond. Whereas during ecodormancy, the cambium remains inactive until favorable external conditions occur, at which point it reactivates. This model provides a potential means to explain our observed connection between BRs and temperatures in February and April, outside of the growth period. In the model, chilling temperatures and forcing temperatures counterbalance each other, and this interaction modulates the onset date of cambial activity. The resulting hypothesis is that the cambium should require a lower accumulation of forcing temperatures during ecodormancy, when it has been exposed to increasingly cold temperatures during the endodormancy phase. Chilling accumulation was modeled to start

shortly after the winter solstice, whereas forcing accumulation starts around the vernal equinox. In the context of our results, this would imply that warmer February temperatures would encompass the chilling accumulation phase and lead to lower chilling temperature accumulation. Further, lower April temperatures shortly after the theoretical start of the forcing accumulation period (vernal equinox), would lead to lower and slower forcing temperature accumulation. This, coupled with higher threshold requirements due to lower chilling accumulation, could lead to later resumption of cambial activity. Consequently, further xylogenesis phases, including lignification, might be delayed towards the end of the growing season, when advection of colder air masses is more likely to occur, further disrupting lignification resulting in underlignified bands of cells in the latewood of a particular year observed as BRs.

Greaves et al. (2022) found only the very strong 1976 BR, present in most of their samples, to be related to a cold end of the growing season. They found the remaining BR years displayed an irregular distribution between and within trees and could not assign these to any specific temperature signal. They concluded that these weaker BRs might be related to other biotic and abiotic stresses. Our modeling approach, based on a long chronology and high sample depth spread along an altitudinal gradient, allowed us to capture a broader picture of interacting thermal conditions during February, April, June, August, September and October, and BR formation modulated by DTL. It is worth noting that the site location studied by Greaves et al. (2022) is not near the thermal limit for Scots pine growth, and therefore the BR signal might have been less consistent. Our samples all come from trees growing close to the temperature-limited upper tree line, where adverse thermal conditions are the main common growth-limiting factor, and BR formation is an observed response to that temperature influence. At different sites, limited by different factors, BR may potentially constitute a compound response to different stressors. Therefore, future studies should target trees coming from a wide range of micro-environmental settings to further assess the consistency of BR formation in trees subjected to different stressors and to aid its ecological interpretation.

4.3 Topographic influence on BR occurrence

Topography influences ring-width patterns in bristlecone pine. Ring widths from the lower forest border correlate with precipitation (Hughes and Funkhouser 1998), whereas at the upper forest border, the correlation is with temperature (LaMarche 1970). The trees used in this study are from the more complex interface zone between the upper and lower tree line (Salzer et al. 2009, 2014b; Kipfmueller and Salzer 2010; Bunn et al. 2011). Ring-width analysis of trees within this zone has shown that near the climatically-determined upper tree line, relatively small differences in elevation of the order of 60–80 vertical meters, alter the factor most limiting to tree-ring growth. Trees growing in a narrow elevational band near the tree line show a pattern of growth consistent with temperature limitation, while trees below this band show a pattern of growth more similar to lower forest border precipitation-sensitive trees. It was also discovered that in a small subset of the trees growing below the upper tree line, but rooted in particular locations on the landscape vulnerable to cold-air pooling, ring-width patterns were more similar to the temperature-sensitive patterns found in the highest trees (Bunn et al. 2011). The BR data in this study add further evidence of this fine-scale spatial sensitivity of bristlecone pine to temperature close to the upper tree line and indicates that this sensitivity may be at even finer scales than previously shown. The BR classification

system developed in this study provided useful additional insights in this context. It revealed that the further below the tree line a tree is located, not only are fewer BRs observed, but those that are, are of lower intensity. Although the microscopic examination of each blue ring occurrence to assign an intensity classification made the analysis more time-consuming, this effort proved to be worthwhile, providing valuable information. It was particularly important to note the presence of even the least intense BR types, BR-3 and BR-4, as these are the more abundant types of this generally rare phenomenon (BR-3 occurred 67 times and BR-4 120 times out of 205 BRs observed for the 1895–2014 period). Omitting these less intense types would lead to ignoring a large portion of the information available from this new proxy. We would recommend that future studies invest in efforts to incorporate BR intensity in their observations, with the caveat that such an approach relies upon a highly standardized and precise thickness of micro-sections to ensure direct comparability of all features.

Outliers from this general DTL dependent pattern, like core NF533B (Fig. 4), which was located in the lower portion of the elevational transect (DTL 116 m) and exhibits a proportion of BRs more consistent with samples from the higher locations, might illustrate the effect of cold air pooling (Bunn et al. 2011). Core NF533B comes from a tree situated on a slight plateau in the NF transect (Fig. 1) which supports this hypothesis. However, cores NF534A and B, from a tree located approximately 10 m from NF533B, both exhibit a much lower proportion of BRs (Fig. 4). It is possible that much larger topographically induced temperature differences experienced by trees exist than previously reported (Bruening 2016; Bruening et al. 2017), or there may be some individual tree level factors, like the genetic susceptibility of particular trees to BR formation, that play a role. The former would be in accordance with the observed lack of regular significant differences between topoclimate variables of trees recording and not recording BRs (Table 3); the latter is supported by observations made for *Pinus radiata* lignification by Donaldson (1993). Work by Salzer et al. (2014b) indicated that trees on the SF slope grew faster than their NF slope counterparts; thus, we expected that SF trees, having somewhat better conditions for growth, might be less responsive in terms of BRs. However, we found no evidence of exposure affecting the probability of BR formation.

Tardif et al. (2020) looked for significant differences in topoclimate variables between BR recording and non-recording trees for 4 BR years they analyzed (536, 1965, 1978, 1982), with sample depth 12, 31, 29, 29 respectively, and found significant differences in elevation, seasonal mean temperature, length of the growing season, and mean May and September temperatures. Our analysis, based on much larger sample depth and including more BR event years than Tardif et al. (2020), shows a much deeper complexity of interactions between topoclimate and BR sensitivity. We observed significant ($p \leq 0.01$) differences only for June in 1907, July 1907, and November 1868 and for DTL in 1907, 1941, 1809, 1837. This shows that the BR sensitivity of particular trees cannot be sufficiently explained by obtained topoclimate variables. In BR event years 1965 and 1982, common for both this study and that of Tardif et al. (2020), contrary to Tardif et al. (2020), we did not find significant differences between any of the analyzed variables. This difference might be due to smaller sample depth analyzed by Tardif et al. (2020) or simply site-specific differences between the White Mountains (this study) and Pearl Peak, Ruby Mountain Range, Nevada (Tardif et al. 2020).

Future studies aimed at constructing the most representative record of BRs possible in bristlecone pine should target trees located close to the upper tree line and involve collection of at least two cores per tree in order to capture a full record of BR years. Trees at lower elevation should also be sampled to provide information about the severity of

particular event years, as the strongest BR events are captured also in trees situated further from the upper tree line.

Additional benefits may be gained from experimental designs to assess the daily temperature thresholds for BR formation; because taking into account that BRs are a very rare phenomenon, it would be very difficult to capture BR formation in observational studies under natural conditions.

A recent study (Björklund et al. 2021), focused on elucidating the differences between different approaches to obtaining maximum latewood density signals (X-ray, Blue Intensity, and quantitative wood anatomy) has shown that incomplete lignification (as represented by BR years) is not captured in X-ray and Blue Intensity methods. We suggest that BR chronologies may have additional value to constitute an independent record of past temperature in the late part of the growing season, not otherwise captured by densitometric techniques. Overall, results demonstrate excellent potential for the future development of BR proxy records from bristlecone pine, and indicate this approach will provide a more sensitive paleotemperature proxy to complement and inform ring width and/or densitometric techniques.

Supplementary Information The online version contains supplementary material available at https://doi.org/10.1007/s10584-024-03773-8

Acknowledgements LS thanks Joanna Karłowska-Pik, Krzysztof Leki and Jakub Wojtasik for useful discussions during the model-building phase of work. The Laboratory of Tree Ring Research is thanked for its support and for making the laboratory facilities available to the leading author during the laboratory preparation phase of work, which took place during the most challenging phase of the COVID pandemic. Heartfelt thanks to the Pearson-Brewer family for the warmest welcome and invaluable support during the research visit.

Authors' contributions L.S. and C.P. conceived the study, M.S. contributed and crossdated the samples, and contributed to manuscript revision, L.S performed laboratory work, conducted analyses, interpretation, visualization and led the writing, N.S-K. contributed to statistical modeling, C.P contributed to interpretation and writing, M.K contributed to manuscript revision.

Funding This work was supported by: National Science Centre 2019/35/N/ST10/04366 to L.S.,
The National Science Foundation's P2C2 program 1902625 and 1203749 to M.S.,
Project nr POWR.03.05.00–00-Z302/17 "Universitas Copernicana Thoruniensis In Futuro" (2018–2022) co-financed from the European Social Fund-the Operational Programme Knowledge Education Development. Module 5. Interdisciplinary PhD School "Academia Copernicana" to L.S.,
The Malcolm H. Wiener Foundation and the University of Arizona to C.P.

Data availability All the data and materials supporting the findings of this study are available from the corresponding author upon reasonable request.

Declarations

Conflict of interest The authors declare that they have no conflict of interest.

References

Baayen RH (2008) Analyzing Linguistic Data: A Practical Introduction to Statistics using R. Cambridge University Press

Barbosa AC, Stahle DW, Burnette DJ, et al (2019) Meteorological Factors Associated With Frost Rings in Rocky Mountain Bristlecone Pine At Mt. Goliath, Colorado. Tree Ring Res 75 101 https://doi.org/10.3959/1536-1098-75.2.101

Bates D, Mächler M, Bolker B, Walker S (2015) Fitting Linear Mixed-Effects Models Using lme4. J Stat Softw 67 https://doi.org/10.18637/jss.v067.i01

Björklund J, Fonti MV, Fonti P et al (2021) Cell wall dimensions reign supreme: cell wall composition is irrelevant for the temperature signal of latewood density/blue intensity in Scots pine. Dendrochronologia (verona) 65:125785

Boyce RL, Lubbers B (2011) Bark-stripping patterns in bristlecone pine (Pinus aristata) stands in Colorado, USA1. J Torrey Bot Soc 138:308–321

Bruening JM, AG, Bunn et al (2017) Fine-scale modeling of bristlecone pine treeline position in the Great Basin, USA. Environ Res Lett 12:14008

Bruening JM, Bunn AG, Salzer MW (2018) A climate-driven tree line position model in the White Mountains of California over the past six millennia. J Biogeogr 45:1067–1076. https://doi.org/10.1111/jbi.13191

Bruening JM (2016) Fine-scale topoclimate modeling and climatic treeline prediction of Great Basin bristlecone pine (Pinus longaeva) in the American southwest

Brunstein FC (1996) Climatic significance of the bristlecone pine latewood frost-ring record at Almagre Mountain, Colorado, U.S.A. Arct Antarct Alp Res 28:65–76. https://doi.org/10.2307/1552087

Brunstein FC (2006) Growth-form characteristics of ancient Rocky Mountain bristlecone pines (Pinus aristata). Colorado. https://doi.org/10.3133/sir20065219

Brunstein FC (1995) Bristlecone pine frost-ring and light-ring chronologies, from 569 BC to AD 1993, Colorado

Bunn AG, Hughes MK, Salzer MW (2011) Topographically modified tree-ring chronologies as a potential means to improve paleoclimate inference: A letter. Clim Change 105:627–634. https://doi.org/10.1007/s10584-010-0005-5

Büntgen U, Crivellaro A, Arseneault D et al (2022) Global wood anatomical perspective on the onset of the Late Antique Little Ice Age (LALIA) in the mid-6th century CE. Sci Bull (beijing) 67:2336–2344. https://doi.org/10.1016/j.scib.2022.10.019

Crivellaro A, Piermattei A, Dolezal J et al (2022) Biogeographic implication of temperature-induced plant cell wall lignification. Commun Biol 5:767. https://doi.org/10.1038/s42003-022-03732-y

Delpierre N, Lireux S, Hartig F et al (2019) Chilling and forcing temperatures interact to predict the onset of wood formation in Northern Hemisphere conifers. Glob Chang Biol 25:1089–1105

Donaldson LA (1991) Seasonal changes in lignin distribution during tracheid development in Pinus radiata D. Don Wood Sci Technol 25:15–24. https://doi.org/10.1007/BF00195553

Donaldson LA (1993) Lignin distribution in wood from a progeny trial of genetically selected Pinus radiata D. Don Wood Sci Technol 27:391–395. https://doi.org/10.1007/BF00192226

Gärtner H, Schweingruber F (2013) Microscopic preparation techniques for plant stem analysis. Verlag Dr, Kessel, Remagen-Oberwinter

Gärtner H, Lucchinetti S, Schweingruber FH (2014) New perspectives for wood anatomical analysis in dendrosciences: The GSL1-microtome. Dendrochronologia (verona) 32:47–51. https://doi.org/10.1016/j.dendro.2013.07.002

Gerlach D (1969) Botanische mikrotechnik. Georg Thieme Verlag

Gindl W, Grabner M, Wimmer R (2000) The influence of temperature on latewood lignin content in treeline Norway spruce compared with maximum density and ring width. Trees - Structure and Function 14:409–414. https://doi.org/10.1007/s004680000057

Glerum C, Farrar JL (1966) Frost Ring Formation in the Stems of Some Coniferous Species. Can J Bot 44:879–886. https://doi.org/10.1139/b66-103

Greaves C, Crivellaro A, Piermattei A et al (2022) Remarkably high blue ring occurrence in Estonian Scots pines in 1976 reveals wood anatomical evidence of extreme autumnal cooling. Trees. https://doi.org/10.1007/s00468-022-02366-1

Gurskaya MA (2014) Temperature conditions of the formation of frost damages in conifer trees in the high latitudes of Western Siberia. Biol Bull 41:187–196

Hughes MK, Funkhouser G (1998) Extremes of moisture availability reconstructed from tree rings for recent millennia in the Great Basin of western North America. The impacts of climate variability on forests 99–107. https://doi.org/10.1007/BFb0009768

Kidd KR, Copenheaver CA, Zink-Sharp A (2014) Frequency and factors of earlywood frost ring formation in jack pine (Pinus banksiana) across northern lower Michigan. Ecoscience 21:157–167
Kipfmueller KF, Salzer MW (2010) Linear trend and climate response of five-needle pines in the western United States related to treeline proximity. Can J for Res 40:134–142
LaMarche VC Jr (1979) (1974) Paleoclimatic Inferences from Long Tree-Ring Records: Intersite comparison shows climatic anomalies that may be linked to features of the general circulation. Science 183:1043–1048. https://doi.org/10.1126/science.183.4129.1043
LaMarche VC, Hirschboeck KK (1984) Frost rings in trees as records of major volcanic eruptions. Nature. https://doi.org/10.1038/307121a0
LaMarche Jr VC (1970) Frost-damage rings in subalpine conifers and their application to tree-ring dating problems. Smith, JH G, and Worrall, J(eds), Tree-ring Analysis with Special Reference to Northwest America University of British Columbia Faculty of Forestry Bulletin 99–100
Matisons R, Gärtner H, Elferts D et al (2020) Occurrence of 'blue' and 'frost' rings reveal frost sensitivity of eastern Baltic provenances of Scots pine. For Ecol Manage 457:117729. https://doi.org/10.1016/j.foreco.2019.117729
Montwé D, Isaac-Renton M, Hamann A, Spiecker H (2018) Cold adaptation recorded in tree rings highlights risks associated with climate change and assisted migration. Nat Commun 9:1–7. https://doi.org/10.1038/s41467-018-04039-5
Payette S, Delwaide A, Simard M (2010) Frost-ring chronologies as dendroclimatic proxies of boreal environments. Geophys Res Lett 37:1–6. https://doi.org/10.1029/2009GL041849
Piermattei A, Crivellaro A, Carrer M, Urbinati C (2015) The "blue ring": anatomy and formation hypothesis of a new tree-ring anomaly in conifers. Trees 29:613–620. https://doi.org/10.1007/s00468-014-1107-x
Piermattei A, Crivellaro A, Krusic PJ et al (2020) A millennium-long 'Blue Ring' chronology from the Spanish Pyrenees reveals severe ephemeral summer cooling after volcanic eruptions. Environ Res Lett 15:124016. https://doi.org/10.1088/1748-9326/abc120
R Core Team (2024) R: A language and environment for statistical computing. R Foundation for Statistical Computing, Vienna, Austria
Saleh TM, Leney L, Sarkanen K V (1967) Radioautographic studies of cottonwood, Douglas fir and wheat plants
Salzer MW, Hughes MK (2007) Bristlecone pine tree rings and volcanic eruptions over the last 5000 yr. Quat Res 67:57–68. https://doi.org/10.1016/j.yqres.2006.07.004
Salzer MW, Hughes MK, Bunn AG, Kipfmueller KF (2009) Recent unprecedented tree-ring growth in bristlecone pine at the highest elevations and possible causes. Proc Natl Acad Sci 106:20348–20353
Salzer MW, Bunn AG, Graham NE, Hughes MK (2014a) Five millennia of paleotemperature from tree-rings in the Great Basin, USA. Clim Dyn 42:1517–1526
Salzer MW, Larson ER, Bunn AG, Hughes MK (2014) Changing climate response in near-treeline bristlecone pine with elevation and aspect. Environ Res Lett 9:114007. https://doi.org/10.1088/1748-9326/9/11/114007
Schulman E (1958) Bristlecone pine, oldest known living thing. Nat Geogr Mag 113:355–372
Schulman E, Ferguson C, (1956) Millenia-old pine trees sampled in 1954 and, (1955). In: Schulman E (ed) Dendroclimatic Changes in Semiarid America. University of Arizona Press, Tucson AZ, pp 136–138
Schweingruber FH (2007) Wood structure and environment. Springer Science \& Business Media
Sigl M, Winstrup M, McConnell JR et al (2015) Timing and climate forcing of volcanic eruptions for the past 2,500 years. Nature 523:543–549. https://doi.org/10.1038/nature14565
Stokes MA (1996) An introduction to tree-ring dating. University of Arizona Press
Tardif JC, Salzer MW, Conciatori F et al (2020) Formation, structure and climatic significance of blue rings and frost rings in high elevation bristlecone pine (Pinus longaeva DK Bailey). Quat Sci Rev 244:106516. https://doi.org/10.1016/j.quascirev.2020.106516
Trendelenburg (1939) Das Holz als Rohstoff. Lehmanns, Munich
Ziaco E, Biondi F, Rossi S, Deslauriers A (2016) Environmental drivers of cambial phenology in Great Basin bristlecone pine. Tree Physiol 36:818–831. https://doi.org/10.1093/treephys/tpw006